

# A structure-preserving numerical method for quasi-incompressible Navier–Stokes–Maxwell–Stefan systems

Aaron Brunk · Ansgar Jüngel · Mária  
Lukáčová-Medviďová

Received: date / Accepted: date

**Abstract** A conforming finite element scheme with mixed explicit–implicit time discretization for quasi-incompressible Navier–Stokes–Maxwell–Stefan systems in a bounded domain with periodic boundary conditions is presented. The system consists of the Navier–Stokes equations, together with a quasi-incompressibility constraint, coupled with the cross-diffusion Maxwell–Stefan equations. The numerical scheme preserves the partial masses and the quasi-incompressibility constraint and dissipates the discrete energy. Numerical experiments in two space dimensions illustrate the convergence of the scheme and the structure-preserving properties.

**Keywords** Quasi-incompressible Navier–Stokes equations · Maxwell–Stefan equations · cross-diffusion systems · finite element method · structure-preserving numerical scheme · discrete mass conservation · energy dissipation

**Mathematics Subject Classification (2020)** 65M60 · 65N30 · 76T30 · 80M10.

## 1 Introduction

Many applications for multicomponent mixtures, like the ion transport in biological channels, the dynamics of electrolytes in lithium-ion batteries, or helium–oxygen–carbon dioxide mixtures in the lung, can be described by Maxwell–Stefan equations. In the Fick–Onsager form, they consist

---

A. J. and M. L.-M. gratefully acknowledge the Research in Teams Fellowship “Entropy methods for evolutionary systems: analysis and numerics” of the Erwin Schrödinger International Institute for Mathematics and Physics, Vienna. A. J. acknowledges partial support from the Austrian Science Fund (FWF), grants 10.55776/F65 and 10.55776/P33010. This work has received funding from the European Research Council (ERC) under the European Union’s Horizon 2020 research and innovation programme, ERC Advanced Grant NEUROMORPH, no. 101018153. The work of M. L.-M. was supported by the Gutenberg Research College and by the Deutsche Forschungsgemeinschaft (DFG, German Research Foundation) – project number 233630050 – TRR 146 and project number 525800857 – SPP 2410 “Hyperbolic Balance Laws: Complexity, Scales and Randomness”. She is also grateful to the Mainz Institute of Multiscale Modelling for supporting her research. A. B. was supported by the Gutenberg Research College and by the DFG – project number 233630050 – TRR 146 and project number 441153493 – SPP 2256 “Variational Methods for Predicting Complex Phenomena in Engineering Structures and Materials”.

---

A. Brunk  
Institute of Mathematics, Johannes Gutenberg-University Mainz, Staudinger Weg 9, 55288 Mainz, Germany  
E-mail: abrunk@uni-mainz.de

A. Jüngel  
Institute of Analysis and Scientific Computing, TU Wien, Wiedner Hauptstraße 8–10, 1040 Wien, Austria  
Erwin Schrödinger International Institute for Mathematics and Physics, Boltzmannngasse 9, 1090 Wien, Austria  
E-mail: juengel@tuwien.ac.at

M. Lukáčová-Medviďová  
Institute of Mathematics, Johannes Gutenberg-University Mainz, Staudinger Weg 9, 55288 Mainz, Germany  
Erwin Schrödinger International Institute for Mathematics and Physics, Boltzmannngasse 9, 1090 Wien, Austria  
E-mail: lukacova@uni-mainz.de

of nonlinear parabolic cross-diffusion equations whose diffusion matrix (called mobility matrix) is positive semidefinite only [4]. In the hydrostatic and isothermal case, the variables are the partial mass densities that satisfy a volume-filling constraint implying a constant total mass density. In the general case, the equations are coupled to the compressible or incompressible Navier–Stokes equations. In this paper, we consider the quasi-incompressible model of [11] and suggest, for the first time, a provable structure-preserving finite element scheme.

### 1.1 Model equations

The model describes the mass transport of the fluid or gas components by convection and diffusion (for the partial mass densities  $\rho_1, \dots, \rho_N$ ) as well as the momentum balance (for the barycentric velocity  $\mathbf{u}$  and the pressure  $p$ ):

$$\partial_t \rho_i + \operatorname{div}(\rho_i \mathbf{u}) + \operatorname{div} \mathbf{J}_i = 0, \quad (1)$$

$$\partial_t(\rho \mathbf{u}) + \operatorname{div}(\rho \mathbf{u} \otimes \mathbf{u} - \mathbb{S}(\vec{\rho}, \nabla \mathbf{u}) + p \mathbb{I}) = 0 \quad \text{in } \Omega, \quad t > 0, \quad (2)$$

$$\rho_i(\cdot, 0) = \rho_i^0, \quad (\rho \mathbf{u})(\cdot, 0) = (\rho \mathbf{u})^0 \quad \text{in } \Omega, \quad i = 1, \dots, N. \quad (3)$$

Here,  $\Omega \subset \mathbb{R}^d$  is a bounded domain (we choose the torus),  $\mathbb{I} \in \mathbb{R}^{N \times N}$  is the unit matrix, the total mass density is defined by  $\rho := \sum_{i=1}^N \rho_i$ , and  $\mathbf{J}_i$  are the diffusion fluxes satisfying the side condition  $\sum_{i=1}^N \mathbf{J}_i = 0$ , which implies after summation of (1) over  $i = 1, \dots, N$  the total mass conservation  $\partial_t \rho + \operatorname{div}(\rho \mathbf{u}) = 0$ . The stress tensor  $\mathbb{S}(\vec{\rho}, \nabla \mathbf{u})$  is assumed to satisfy the coercivity condition  $\mathbb{S}(\vec{\rho}, \nabla \mathbf{u}) : \nabla \mathbf{u} \geq 0$ , where “:” is the Frobenius matrix product (summation over both indices). A typical example is  $\mathbb{S}(\vec{\rho}, \nabla \mathbf{u}) = \nu(\nabla \mathbf{u}^T + \nabla \mathbf{u}) + \lambda(\operatorname{div} \mathbf{u})\mathbb{I}$ , where  $\nu > 0$  and  $\lambda \geq -\frac{2}{d}\nu$  may depend on the density vector  $\vec{\rho} := (\rho_1, \dots, \rho_N)$ , and the coercivity condition follows from Korn’s inequality [13, Sec. 10.9].

The partial diffusion flux is given as the linear combination of the gradients of the chemical potentials  $\mu_i$ ,

$$\mathbf{J}_i = - \sum_{j=1}^N M_{ij}(\vec{\rho}) \nabla \mu_j, \quad i = 1, \dots, N. \quad (4)$$

The mobility (or Onsager) matrix  $M = (M_{ij})_{i,j=1}^N \in \mathbb{R}^{N \times N}$  is assumed to be symmetric and positive semi-definite satisfying  $\sum_{j=1}^N M_{ij}(\vec{\rho}) = 0$  for all  $\vec{\rho} \in [0, \infty)^N$ . This condition is consistent with the side condition of vanishing net diffusion flux. If all Maxwell–Stefan diffusion coefficients are equal, the mobility matrix has the entries

$$M_{ij}(\vec{\rho}) = \rho_i \delta_{ij} - \frac{\rho_i \rho_j}{\rho}, \quad i, j = 1, \dots, N. \quad (5)$$

We use this expression in our numerical experiments, but the numerical analysis does not rely on this choice. The chemical potentials  $\mu_i$  are defined by

$$\mu_i = \frac{\partial f}{\partial \rho_i}(\vec{\rho}) + V_i p, \quad i = 1, \dots, N, \quad (6)$$

where  $f$  is the internal energy density and  $V_i > 0$  are the specific volumes of the molecules. A typical example for ideal gas mixtures is given by  $f(\vec{\rho}) = \sum_{i=1}^N \rho_i \log(\rho_i/\rho)$ , used for the numerical tests. Note that our numerical analysis holds for general energy densities that are positively homogeneous of degree one. The incompressibility constraint is imposed by

$$\sum_{i=1}^N V_i \rho_i = 1. \quad (7)$$

Observe that definition (6) is consistent with the Gibbs–Duhem relation

$$-f(\vec{\rho}) + \sum_{i=1}^N \rho_i \mu_i = - \sum_{i=1}^N \rho_i \frac{\partial f}{\partial \rho_i} + \sum_{i=1}^N \rho_i \mu_i = \sum_{i=1}^N \rho_i V_i p = p,$$

where the first identity follows from the positive homogeneity of  $f$  and the last identity is a consequence of (7).

In the case of equal specific volumes  $V_i = V > 0$  for all  $i = 1, \dots, N$ , we recover the volume-filling condition  $\sum_{i=1}^N \rho_i = 1/V$ , which implies from mass conservation (1) the standard divergence-free condition  $\operatorname{div} \mathbf{u} = 0$ . This yields the incompressible Navier–Stokes equations

$$V^{-1} \partial_t \mathbf{u} + \operatorname{div}(V^{-1} \mathbf{u} \otimes \mathbf{u} - \mathbb{S}(\vec{\rho}, \nabla \mathbf{u}) + p \mathbb{I}) = 0, \quad \operatorname{div} \mathbf{u} = 0, \quad (8)$$

that are decoupled from the Maxwell–Stefan equations; see, e.g., [9, 23].

In the general case, we multiply (1) by  $V_i$  and sum over  $i = 1, \dots, N$ :

$$0 = \partial_t \left( \sum_{i=1}^N V_i \rho_i \right) + \operatorname{div} \left( \sum_{i=1}^N V_i \rho_i \mathbf{u} \right) + \operatorname{div} \left( \sum_{i=1}^N V_i \mathbf{J}_i \right) = \operatorname{div} \mathbf{u} + \operatorname{div} \left( \sum_{i=1}^N V_i \mathbf{J}_i \right), \quad (9)$$

which is interpreted as a quasi-incompressibility constraint. In particular, a net local change of volume is possible because of mixing. Summarizing, we can formulate our system (1)–(7) as

$$\partial_t \rho_i + \operatorname{div}(\rho_i \mathbf{u}) - \operatorname{div} \left( \sum_{i,j=1}^N M_{ij}(\vec{\rho}) \nabla \mu_j \right) = 0, \quad (10)$$

$$\partial_t(\rho \mathbf{u}) + \operatorname{div}(\rho \mathbf{u} \otimes \mathbf{u} - \mathbb{S}(\vec{\rho}, \nabla \mathbf{u}) + p \mathbb{I}) = 0, \quad (11)$$

$$\mu_i = \frac{\partial f}{\partial \rho_i} + V_i p, \quad i = 1, \dots, N, \quad (12)$$

$$\operatorname{div} \mathbf{u} = \operatorname{div} \left( \sum_{i,j=1}^N V_i M_{ij}(\vec{\rho}) \nabla \mu_j \right). \quad (13)$$

## 1.2 Main results

The aim of this paper is the design of a structure-preserving finite element method for system (10)–(13). In particular, the numerical scheme preserves the partial masses and the quasi-incompressibility constraint (7), conserves the total mass, and satisfies an energy inequality. The energy density of the system is given by the sum of the kinetic and internal energy densities,

$$E(\vec{\rho}, \mathbf{u}) = \frac{\rho}{2} |\mathbf{u}|^2 + f(\vec{\rho}). \quad (14)$$

We show in Lemma 3 that the following energy identity holds for smooth solutions:

$$\frac{d}{dt} \int_{\Omega} E(\vec{\rho}, \mathbf{u}) dx + \int_{\Omega} \left( \mathbb{S}(\vec{\rho}, \nabla \mathbf{u}) : \nabla \mathbf{u} + \sum_{i,j=1}^N M_{ij}(\vec{\rho}) \nabla \mu_i \cdot \nabla \mu_j \right) dx = 0.$$

We prove two main results. First, with  $(\rho_{h,i}^k, \mathbf{u}_h^k)$  being the finite element approximation of  $(\rho_i, \mathbf{u})$  at time  $t_k = k\tau$  (with time step  $\tau > 0$ ), we show in Theorem 1 that the discrete partial masses are preserved and that the discrete energy density  $E_h^k = \frac{1}{2} \rho_h^k |\mathbf{u}_h^k|^2 + f(\vec{\rho}_h^k)$  (with  $\rho_h^k := \sum_{i=1}^N \rho_{h,i}^k$ ) satisfies

$$\frac{1}{\tau} \int_{\Omega} (E_h^{k+1} - E_h^k) dx$$

$$= - \int_{\Omega} \left( \mathbb{S}(\vec{\rho}_h^*, \nabla \mathbf{u}_h^{k+1}) : \nabla \mathbf{u}_h^{k+1} + \sum_{i,j=1}^N M_{ij}(\vec{\rho}_h^*) \nabla \mu_{h,i}^{k+1} \cdot \nabla \mu_{h,j}^{k+1} \right) dx - \mathcal{D}_{\text{num}} \leq 0,$$

where  $\rho_{h,i}^*$  depends on  $(\rho_{h,j}^k, \rho_{h,i}^{k+1})$  and  $\mu_{h,i}^{k+1}$  is the discrete chemical potential. The numerical dissipation  $\mathcal{D}_{\text{num}}$  is nonnegative and depends on the discrete kinetic defect and the Hessian of the internal energy density.

Second, we prove that the constraint  $\sum_{i=1}^N V_i \rho_{h,i}^k = 1$  holds pointwise in  $\Omega$  and that the discrete total mass density is strictly positive; see Theorem 2.

The discrete energy inequality yields some a priori bounds detailed in Theorem 2. However, the existence of a discrete solution to scheme (10)–(13) is still an open problem. The existence of a global weak solution to the continuous problem in a bounded domain with Neumann boundary conditions was shown in [11]. The pressure turns out to be a measure with singular values at the minimal and maximal values of the total mass density. Thus, it is not clear to what extent the analysis of [11] can be applied to the finite element case. Another approach is the local-in-time existence result of [3], which yields an integrable pressure function. The idea of the proof is a reformulation of the problem in terms of so-called relative chemical potentials and the construction of a fixed point mapping. As the arguments are quite involved, it is not known whether the arguments hold in the finite-dimensional case.

### 1.3 State of the art

The existence of global weak solutions to the incompressible Navier–Stokes–Maxwell–Stefan equations (i.e.  $V_i = V$  for  $i = 1, \dots, N$ ) was shown in [5, 9, 10, 23]. Existence results for the quasi-incompressible model (i.e. for general  $V_i > 0$ ) were presented in [3, 11]. Analytical results for quasi-incompressible fluids, related but different to (7), can be found in, e.g., [12, 16]. In [16], a mass conservative and energy dissipative discontinuous Galerkin finite element discretization for quasi-incompressible Navier–Stokes–Cahn–Hilliard systems was presented. We have only found the work [1] regarding numerical approximations of coupled Maxwell–Stefan fluid models, where a finite element method for coupling the steady-state Maxwell–Stefan equations to compressible Stokes flow was proposed. Thus, structure-preserving numerical methods for quasi-incompressible Navier–Stokes–Maxwell–Stefan systems are missing in the literature.

The literature is much richer for the Maxwell–Stefan equations with vanishing barycentric velocity. The existence of weak solutions was proved in [2, 15, 20], and the analysis for heat-conducting flows was investigated in [17, 19]. Numerical works include explicit Euler finite difference schemes in one space dimension [6], iterative solvers for such discretizations [14], and mixed finite element methods [24]. More recently, numerical approximations focused on structure-preserving schemes. In [18], an energy-stable and positivity-preserving IMEX finite difference discretization was proposed, based on an equivalent optimization problem. The work [8] suggested a convergent finite volume method that preserves the non-negativity of the densities, the mass conservation, and the volume-filling constraint. For general cross-diffusion equations, including the Maxwell–Stefan systems, structure-preserving schemes were investigated in [7] (Galerkin approximation) and [21] (finite volume discretization).

The paper is organized as follows. We derive in Section 2 various formulations of our model and show the energy identity. The numerical scheme and its structure-preserving properties are proved in Section 3. This section contains our main analytical results. Finally, in Section 4, we present some numerical experiments.

## 2 Various formulations

We introduce the following notation. Vectors in  $\mathbb{R}^N$  are written as  $\vec{v}$ , while vectors in  $\mathbb{R}^d$  are denoted by  $\mathbf{v}$ . Matrices are formulated as  $\mathbb{M}$ . The  $L^2(\Omega)$  inner product is denoted by  $\langle \cdot, \cdot \rangle$ , and we set  $\mathbf{1} = (1, \dots, 1)^T \in \mathbb{R}^N$ . We impose the following assumptions:

- (A0) Domain:  $\Omega = \mathbb{T}^d$  is the  $d$ -dimensional torus,  $d \geq 1$ .  
(A1) Mobility matrix:  $\mathbb{M}(\vec{\rho}) = (M_{ij}(\vec{\rho}))_{i,j=1}^N \in (0, \infty)^{N \times N}$  is symmetric positive semi-definite.  
(A2) Internal energy density:  $f : [0, \infty)^N \rightarrow \mathbb{R}^N$  is smooth and positively homogeneous of degree one.  
(A3) Viscous stress tensor:  $\mathbb{S} : [0, \infty)^N \times \mathbb{R}^{d \times d} \rightarrow \mathbb{R}^{d \times d}$  satisfies  $\mathbb{S}(\vec{\rho}, \nabla \mathbf{u}) : \nabla \mathbf{u} \geq c_S |\nabla \mathbf{u}|^2$  for all  $\nabla \mathbf{u} \in \mathbb{R}^{d \times d}$  and for some  $c_S > 0$ .  
(A4) Initial data and specific volumes:  $\rho_i^0 \geq 0$  and  $(\rho \mathbf{u})^0$  are integrable functions. It holds that  $\sum_{i=1}^N V_i \rho_i^0 = 1$  in  $\Omega$ , where  $V_i > 0$  for  $i = 1, \dots, N$ .

We call a function  $f$  positively homogeneous of degree one if  $f(\lambda \vec{\rho}) = \lambda f(\vec{\rho})$  for all  $\lambda > 0$  and  $\vec{\rho} \in [0, \infty)^N$ . By Euler's homogeneous function theorem, any positively homogeneous function  $f$  of degree one satisfies  $f(\vec{\rho}) = \sum_{i=1}^N \rho_i \partial f / \partial \rho_i$ . This implies, for smooth functions  $\vec{\rho} = \vec{\rho}(x)$ , that

$$\sum_{i=1}^N \rho_i \nabla \frac{\partial f}{\partial \rho_i} = \nabla \sum_{i=1}^N \rho_i \frac{\partial f}{\partial \rho_i} - \sum_{i=1}^N \nabla \rho_i \frac{\partial f}{\partial \rho_i} = \nabla \sum_{i=1}^N \rho_i \frac{\partial f}{\partial \rho_i} - \nabla f(\vec{\rho}) = 0. \quad (15)$$

Observe that any positively homogeneous function is convex (but not strictly convex).

**Lemma 1 (Reformulation)** *Equations (1)–(4), (6)–(7) can be written as (10)–(13) for smooth solutions. If  $V_i = V > 0$  for  $i = 1, \dots, N$ , equations (11) and (13) reduce to (8).*

*Proof* Relation (13) follows from the computation in (9), proving the first assertion. If  $V_i = V$ , it follows from  $\sum_{i=1}^N M_{ij}(\vec{\rho}) = 0$  that  $\sum_{i=1}^N \mathbf{J}_i = 0$  and hence  $\operatorname{div} \mathbf{u} = 0$ . Since  $\rho = V^{-1}$ , we obtain equations (8).

**Lemma 2 (Positivity of the mass densities)** *Let  $f(\vec{\rho}) = \sum_{i=1}^N \rho_i \log(\rho_i/\rho)$  and let  $(\vec{\rho}, \vec{\mu}, \mathbf{u}, p)$  be a smooth solution to (1)–(4), (6)–(7). Then  $\rho_i(t) > 0$  in  $\Omega$ ,  $t > 0$ ,  $i = 1, \dots, N$ .*

*Proof* We deduce from (12) and the explicit expression of  $f$  that  $\rho_i/\rho = \exp(\mu_i - V_i p)$ . Then, multiplying this expression by  $V_i$ , summing over  $i = 1, \dots, N$ , and using the constraint (7), we obtain  $1/\rho = \sum_{i=1}^N V_i \rho_i/\rho = \sum_{i=1}^N V_i \exp(\mu_i - V_i p) > 0$ . This implies that  $\rho > 0$  and consequently,  $\rho_i = \rho \exp(\mu_i - V_i p) > 0$ .

**Lemma 3 (Energy identity)** *It holds for smooth solutions to (1)–(4) that*

$$\frac{d}{dt} \int_{\Omega} E(\vec{\rho}, \mathbf{u}) dx + \int_{\Omega} \left( \mathbb{S}(\vec{\rho}, \nabla \mathbf{u}) : \nabla \mathbf{u} + \sum_{i,j=1}^N M_{ij}(\vec{\rho}) \nabla \mu_i \cdot \nabla \mu_j \right) dx = 0,$$

where the energy density  $E$  is defined in (14).

*Proof* We compute:

$$\frac{d}{dt} \int_{\Omega} E(\vec{\rho}, \mathbf{u}) dx = \int_{\Omega} \left( \frac{1}{2} \partial_t \rho |\mathbf{u}|^2 + \rho \mathbf{u} \cdot \partial_t \mathbf{u} + \sum_{i=1}^N \frac{\partial f}{\partial \rho_i} \partial_t \rho_i \right) dx.$$

It follows from  $\sum_{i=1}^N \mathbf{J}_i = 0$  that  $\partial_t \rho = -\operatorname{div}(\rho \mathbf{u})$  and

$$\rho \partial_t \mathbf{u} = \partial_t(\rho \mathbf{u}) - \mathbf{u} \partial_t \rho = -\operatorname{div}(\rho \mathbf{u} \otimes \mathbf{u} - \mathbb{S}(\vec{\rho}, \nabla \mathbf{u}) + p \mathbb{I}) + \mathbf{u} \operatorname{div}(\rho \mathbf{u}).$$

Inserting the mass and momentum balance equations and integrating by parts, this shows that

$$\begin{aligned} \frac{d}{dt} \int_{\Omega} E(\vec{\rho}, \mathbf{u}) dx &= \int_{\Omega} \left( -\frac{1}{2} |\mathbf{u}|^2 \operatorname{div}(\rho \mathbf{u}) - \operatorname{div}(\rho \mathbf{u} \otimes \mathbf{u} - \mathbb{S}(\vec{\rho}, \nabla \mathbf{u}) + p \mathbb{I}) \mathbf{u} + |\mathbf{u}|^2 \operatorname{div}(\rho \mathbf{u}) \right. \\ &\quad \left. - \sum_{i=1}^N \frac{\partial f}{\partial \rho_i} \operatorname{div}(\rho_i \mathbf{u} + \mathbf{J}_i) \right) dx \end{aligned}$$

$$\begin{aligned}
&= \int_{\Omega} \left( \rho \mathbf{u} \cdot \nabla \mathbf{u} \cdot \mathbf{u} + (\rho \mathbf{u} \otimes \mathbf{u} - \mathbb{S}(\vec{\rho}, \nabla \mathbf{u}) + p \mathbb{I}) : \nabla \mathbf{u} - 2\rho \mathbf{u} \cdot \nabla \mathbf{u} \cdot \mathbf{u} \right. \\
&\quad \left. + \sum_{i=1}^N (\rho_i \mathbf{u} + \mathbf{J}_i) \cdot \nabla \frac{\partial f}{\partial \rho_i} \right) dx \\
&= \int_{\Omega} \left( -\mathbb{S}(\vec{\rho}, \nabla \mathbf{u}) : \nabla \mathbf{u} + p \operatorname{div} \mathbf{u} + \sum_{i=1}^N \rho_i \nabla \frac{\partial f}{\partial \rho_i} \cdot \mathbf{u} + \sum_{i=1}^n \mathbf{J}_i \cdot \nabla \frac{\partial f}{\partial \rho_i} \right) dx.
\end{aligned}$$

It follows from (15) that the third term on the right-hand side vanishes. Inserting the definition of  $\mathbf{J}_i$  and observing that  $\partial f / \partial \rho_i = \mu_i - p V_i$ , we find that

$$\frac{d}{dt} \int_{\Omega} E(\vec{\rho}, \mathbf{u}) dx = \int_{\Omega} \left( -\mathbb{S}(\vec{\rho}, \nabla \mathbf{u}) : \nabla \mathbf{u} + p \operatorname{div} \mathbf{u} - \sum_{i,j=1}^N M_{ij} \nabla \mu_j \cdot \nabla \mu_i - \sum_{i=1}^N V_i \mathbf{J}_i \cdot \nabla p \right) dx,$$

and by (13), the second and fourth terms on the right-hand side cancel.  $\square$

For the following result, we introduce the skew-symmetric bilinear form

$$(\mathbf{v}, \mathbf{w}) \mapsto \mathbf{b}_{\text{skw}}(\rho \mathbf{u}; \mathbf{v}, \mathbf{w}) = \frac{1}{2} (\langle (\rho \mathbf{u} \cdot \nabla) \mathbf{v}, \mathbf{w} \rangle - \langle (\rho \mathbf{u} \cdot \nabla) \mathbf{w}, \mathbf{v} \rangle).$$

**Lemma 4 (Variational formulation)** *Smooth solutions  $(\vec{\rho}, \vec{\mu}, \mathbf{u}, p)$  to (1)–(4), (6)–(7) satisfy the following variational equations:*

$$\langle \partial_t \rho_i, \psi_i \rangle - \langle \rho_i \mathbf{u}, \psi_i \rangle + \sum_{j=1}^N \langle M_{ij}(\vec{\rho}) \nabla \mu_j, \nabla \psi_i \rangle = 0, \quad (16)$$

$$\langle \mu_i, \xi_i \rangle - \left\langle \frac{\partial f}{\partial \rho_i}(\vec{\rho}) + V_i p, \xi_i \right\rangle = 0, \quad i = 1, \dots, N, \quad (17)$$

$$\frac{1}{2} \langle \mathbf{u} \partial_t \rho, \mathbf{v} \rangle + \langle \rho \partial_t \mathbf{u}, \mathbf{v} \rangle - \mathbf{b}_{\text{skw}}(\rho \mathbf{u}; \mathbf{u}, \mathbf{v}) \quad (18)$$

$$- \langle p, \operatorname{div} \mathbf{v} \rangle + \langle \mathbb{S}((\vec{\rho}, \nabla \mathbf{u})), \nabla \mathbf{v} \rangle + \sum_{i=1}^N \langle \rho_i \nabla (\mu_i - V_i p), \mathbf{v} \rangle = 0,$$

$$\langle \operatorname{div} \mathbf{u}, q \rangle = - \sum_{i,j=1}^N \langle V_i M_{ij}(\vec{\rho}) \nabla \mu_j, \nabla q \rangle \quad (19)$$

for all smooth test functions  $(\psi_i, \xi_i, \mathbf{v}, q)$ ,  $i = 1, \dots, N$ .

*Proof* Equations (16), (17), and (19) follow directly from (10), (11), and (13), respectively, after multiplication with a test function and integration by parts. We only need to show that (18) follows from the momentum equation (11). To this end, we multiply (11) by a test function  $\mathbf{v}$  and integrate by parts:

$$0 = \langle \partial_t(\rho \mathbf{u}), \mathbf{v} \rangle + \langle \operatorname{div}(\rho \mathbf{u} \otimes \mathbf{u}), \mathbf{v} \rangle + \langle \mathbb{S}((\vec{\rho}, \nabla \mathbf{u})), \nabla \mathbf{v} \rangle - \langle p, \operatorname{div} \mathbf{v} \rangle.$$

Using the mass balance equation  $\partial_t \rho = -\operatorname{div}(\rho \mathbf{u})$  and integrating by parts, the first two terms can be written as

$$\begin{aligned}
&\langle \partial_t(\rho \mathbf{u}), \mathbf{v} \rangle + \langle \operatorname{div}(\rho \mathbf{u} \otimes \mathbf{u}), \mathbf{v} \rangle = \langle \mathbf{u} \partial_t \rho, \mathbf{v} \rangle + \langle \rho \partial_t \mathbf{u}, \mathbf{v} \rangle + \langle \operatorname{div}(\rho \mathbf{u} \otimes \mathbf{u}), \mathbf{v} \rangle \\
&= \frac{1}{2} \langle \mathbf{u} \partial_t \rho, \mathbf{v} \rangle - \frac{1}{2} \langle \mathbf{u} \operatorname{div}(\rho \mathbf{u}), \mathbf{v} \rangle + \langle \rho \partial_t \mathbf{u}, \mathbf{v} \rangle + \langle \operatorname{div}(\rho \mathbf{u} \otimes \mathbf{u}), \mathbf{v} \rangle \\
&= \frac{1}{2} \langle \mathbf{u} \partial_t \rho, \mathbf{v} \rangle + \frac{1}{2} (\langle \rho(\mathbf{u} \cdot \nabla) \mathbf{u}, \mathbf{v} \rangle + \langle \rho(\mathbf{u} \cdot \nabla) \mathbf{v}, \mathbf{u} \rangle) + \langle \rho \partial_t \mathbf{u}, \mathbf{v} \rangle - \langle \rho(\mathbf{u} \cdot \nabla) \mathbf{u}, \mathbf{v} \rangle \\
&= \frac{1}{2} \langle \mathbf{u} \partial_t \rho, \mathbf{v} \rangle + \langle \rho \partial_t \mathbf{u}, \mathbf{v} \rangle - \frac{1}{2} (\langle \rho(\mathbf{u} \cdot \nabla) \mathbf{u}, \mathbf{v} \rangle - \langle \rho(\mathbf{u} \cdot \nabla) \mathbf{v}, \mathbf{u} \rangle)
\end{aligned}$$

$$= \frac{1}{2} \langle \mathbf{u} \partial_t \rho, \mathbf{v} \rangle + \langle \rho \partial_t \mathbf{u}, \mathbf{v} \rangle - \mathbf{b}_{\text{skw}}(\rho \mathbf{u}; \mathbf{u}, \mathbf{v}).$$

Adding the equation

$$\begin{aligned} 0 &= \sum_{i=1}^N (\langle \rho_i \nabla \mu_i, \mathbf{v} \rangle + \langle \mu_i, \operatorname{div}(\rho_i \mathbf{v}) \rangle) \\ &= \sum_{i=1}^N \left( \langle \rho_i \nabla \mu_i, \mathbf{v} \rangle + \left\langle \frac{\partial f}{\partial \rho_i} + V_i p, \operatorname{div}(\rho_i \mathbf{v}) \right\rangle \right) \\ &= \sum_{i=1}^N \left( \langle \rho_i \nabla \mu_i, \mathbf{v} \rangle - \left\langle \rho_i \nabla \frac{\partial f}{\partial \rho_i}, \mathbf{v} \right\rangle - \langle \nabla p, V_i \rho_i \mathbf{v} \rangle \right) \\ &= \sum_{i=1}^N \langle \rho_i \nabla (\mu_i - V_i p), \mathbf{v} \rangle \end{aligned}$$

yields our claim (18).  $\square$

In the following section, we suggest a discrete finite element version of the previous variational formulation.

### 3 Numerical analysis

#### 3.1 Numerical scheme

We partition the time interval  $[0, T]$  uniformly into  $n$  subintervals  $[t_{k-1}, t_k]$ , where  $t_k = k\tau$ ,  $k = 1, \dots, n$ , and  $\tau = T/n$  is the time step size. We introduce

$$\begin{aligned} \Pi_\tau^0(\mathcal{U}) &= \text{space of continuous piecewise constant functions on } \{t_0, \dots, t_n\} \\ &\quad \text{with values in } \mathcal{U}, \end{aligned}$$

$$\Pi_\tau^1(\mathcal{U}) = \text{space of piecewise linear functions on } \{t_0, \dots, t_n\} \text{ with values in } \mathcal{U}.$$

For the spatial discretization, we require that  $\mathcal{T}_h$  is a geometrically conforming partition of  $\Omega$  into simplices that can be extended periodically to periodic extensions of  $\Omega$ , with  $h > 0$  being the maximal diameter of the simplices. In particular, the boundary of  $\Omega$  coincides with the boundary of the triangulation. Let  $P_k(K)$  be the space of polynomials with maximal degree  $k \in \mathbb{N}$  on  $K \in \mathcal{T}_h$ . We define the spaces of piecewise linear and quadratic functions by, respectively,

$$\begin{aligned} \mathcal{V}_h &= \{v \in H^1(\Omega) \cap C^0(\overline{\Omega}) : v|_K \in P_1(K) \text{ for all } K \in \mathcal{T}_h\}, \\ \mathcal{X}_h &= \{v \in H^1(\Omega) \cap C^0(\overline{\Omega}) : v|_K \in P_2(K) \text{ for all } K \in \mathcal{T}_h\}, \end{aligned}$$

and the spaces of mean-free and positive functions, respectively,

$$\mathcal{Q}_h = \{v \in \mathcal{V}_h : \langle v, 1 \rangle = 0\}, \quad \mathcal{V}_{h,+} = \{v \in \mathcal{V}_h : v(x) > 0 \text{ for } x \in \Omega\},$$

recalling that  $\langle u, v \rangle = \sum_{K \in \mathcal{T}_h} u|_K v|_K$ .

Let the initial data  $(\bar{\rho}_h^0, \mathbf{u}_h^0) \in \mathcal{V}_{h,+}^N \times \mathcal{X}_h^d$  be given. The numerical scheme reads as follows: Find  $(\bar{\rho}_h^k, \mathbf{u}_h^k) \in \Pi_\tau^1(\mathcal{V}_{h,+}^N \times \mathcal{X}_h^d)$  and  $(\bar{\mu}_h^k, p_h^k) \in \Pi_\tau^0(\mathcal{V}_h^N \times \mathcal{Q}_h)$  for  $k = 0, \dots, n-1$  such that for  $i = 1, \dots, N$ ,

$$\frac{1}{\tau} \langle \rho_{h,i}^{k+1} - \rho_{h,i}^k, \psi_i \rangle - \langle \rho_{h,i}^k \mathbf{u}_h^{k+1}, \nabla \psi_i \rangle + \sum_{j=1}^N \langle M_{ij}(\bar{\rho}_h^*) \nabla \mu_{h,j}^{k+1}, \nabla \psi_i \rangle = 0, \quad (20)$$

$$\langle \mu_{h,i}^{k+1}, \xi_i \rangle - \left\langle \frac{\partial f}{\partial \rho_i}(\bar{\rho}_h^{k+1}) + V_i p_h^{k+1}, \xi_i \right\rangle = 0, \quad (21)$$

$$\frac{1}{2\tau} \langle \mathbf{u}_h^{k+1} (\rho_h^{k+1} - \rho_h^k), \mathbf{v} \rangle + \frac{1}{\tau} \langle \rho_h^k (\mathbf{u}_h^{k+1} - \mathbf{u}_h^k), \mathbf{v} \rangle + \mathbf{b}_{\text{skw}}(\rho_h^* \mathbf{u}_h^*; \mathbf{u}_h^{k+1}, \mathbf{v}) \quad (22)$$

$$- \langle p_h^{k+1}, \text{div} \mathbf{v} \rangle + \langle \mathbb{S}(\bar{\rho}_h^*, \nabla \mathbf{u}_h^{k+1}), \nabla \mathbf{v} \rangle + \sum_{i=1}^N \langle \rho_{h,i}^k \nabla (\mu_{h,i}^{k+1} - V_i p_h^{k+1}), \mathbf{v} \rangle = 0,$$

$$\langle \text{div} \mathbf{u}_h^{k+1}, q \rangle = - \sum_{i,j=1}^N \langle V_i M_{ij}(\bar{\rho}_h^*) \nabla \mu_{h,j}^{k+1}, \nabla q \rangle \quad (23)$$

for all  $(\psi_i, \xi_i, \mathbf{v}, q) \in \mathcal{V}_h^N \times \mathcal{V}_h^N \times \mathcal{X}_h^d \times \mathcal{Q}_h$ . Here,  $\rho_h^*$  and  $\mathbf{u}_h^*$  are functions of  $(\rho_h^k, \rho_h^{k+1})$  and  $(\mathbf{u}_h^k, \mathbf{u}_h^{k+1})$ , respectively. Examples are the explicit scheme  $(\rho_h^*, \mathbf{u}_h^*) = (\rho_h^k, \mathbf{u}_h^k)$ , the implicit scheme  $(\rho_h^*, \mathbf{u}_h^*) = (\rho_h^{k+1}, \mathbf{u}_h^{k+1})$ , or the mid-point rule. In the numerical experiments, we have chosen the explicit approximation. The discrete pressure terms in (22) encode the incompressibility condition (7). In fact, if (7) holds, these terms cancel out.

We mentioned already in the introduction that we assume the existence of a discrete solution to (20)–(23), since a proof is far from being trivial. In particular, we assume that  $\rho_{h,i}^k$  is nonnegative for  $i = 1, \dots, N$  and  $k = 1, \dots, n$ . This is consistent with the continuous model; see Lemma 2.

### 3.2 Properties of the numerical scheme

The following numerical properties hold.

**Theorem 1 (Discrete identities)** *Let Assumptions (A0) – (A4) hold. Every discrete solution  $(\bar{\rho}_h^k, \mathbf{u}_h^k) \in \Pi_\tau^1(\mathcal{V}_{h,+}^N \times \mathcal{X}_h^d)$ ,  $(\bar{\mu}_h^k, p_h^k) \in \Pi_\tau^0(\mathcal{V}_h^N \times \mathcal{Q}_h)$  to (20)–(23) satisfies the following identities for  $k \in \{0, \dots, n-1\}$ .*

– *Partial mass conservation: For all  $i = 1, \dots, N$ ,*

$$\langle \rho_{h,i}^{k+1}, 1 \rangle = \langle \rho_{h,i}^k, 1 \rangle.$$

– *Total mass conservation equation: For all  $q \in \mathcal{V}_h$ ,*

$$\frac{1}{\tau} \langle \rho_h^{k+1} - \rho_h^k, q \rangle - \langle \rho_h^k \mathbf{u}_h^{k+1}, \nabla q \rangle = 0.$$

– *Constraint: For all  $q \in \mathcal{Q}_h$ ,*

$$\frac{1}{\tau} \left\langle \sum_{i=1}^N V_i \rho_{h,i}^{k+1} - 1, q \right\rangle - \frac{1}{\tau} \left\langle \sum_{i=1}^N V_i \rho_{h,i}^k - 1, q \right\rangle = \left\langle \left( \sum_{i=1}^N V_i \rho_{h,i}^k - 1 \right) \mathbf{u}_h^{k+1}, \nabla q \right\rangle. \quad (24)$$

– *Discrete energy equality:*

$$\begin{aligned} & \frac{1}{\tau} \langle E_h^{k+1} - E_h^k, 1 \rangle \\ &= - \langle \mathbb{S}(\bar{\rho}_h^*, \nabla \mathbf{u}_h^{k+1}), \nabla \mathbf{u}_h^{k+1} \rangle - \sum_{i,j=1}^N \langle M_{ij}(\bar{\rho}_h^*) \nabla \mu_{h,i}^{k+1}, \nabla \mu_{h,j}^{k+1} \rangle - \mathcal{D}_{\text{num}} \leq 0, \end{aligned}$$

where the discrete energy density and numerical dissipation are given by

$$E_h^k = \frac{1}{2} \rho_h^k |\mathbf{u}_h^k|^2 + f(\bar{\rho}_h^k),$$

$$\mathcal{D}_{\text{num}} = \frac{1}{2\tau} \|(\rho_h^k)^{1/2} (\mathbf{u}_h^{k+1} - \mathbf{u}_h^k)\|_{L^2(\Omega)}^2 + \frac{1}{\tau} \sum_{i,j=1}^N \left\langle \frac{\partial^2 f}{\partial \rho_i \partial \rho_j}(\bar{\omega}_h) (\rho_{h,i}^{k+1} - \rho_{h,i}^k), \rho_{h,j}^{k+1} - \rho_{h,j}^k \right\rangle,$$

and  $\bar{\omega}_h$  is a convex combination of  $\bar{\rho}_h^k$  and  $\bar{\rho}_h^{k+1}$ .

*Proof* The conservation of the partial masses is obtained by choosing  $\psi_i = 1$  in (20). The sum of (20) over  $i = 1, \dots, N$  with  $\psi_i = q$  and the fact that  $\sum_{i=1}^N M_{ij}(\bar{\rho}_h) = 0$  leads to the total mass conservation equation. The equation for the constraint follows from (20) by choosing  $\psi_i = V_i q \in \mathcal{V}_h$  for  $q \in \mathcal{Q}_h$  (hence  $\langle q, 1 \rangle = 0$ ), summing over  $i = 1, \dots, N$ , and using (23):

$$\begin{aligned} & \frac{1}{\tau} \left\langle \sum_{i=1}^N V_i \rho_{h,i}^{k+1} - 1, q \right\rangle - \frac{1}{\tau} \left\langle \sum_{i=1}^N V_i \rho_{h,i}^k - 1, q \right\rangle \\ &= \left\langle \sum_{i=1}^N V_i \rho_{h,i}^k \mathbf{u}_h^{k+1}, \nabla q \right\rangle + \left\langle \sum_{i=1}^N V_i \mathbf{J}_{h,i}^{k+1}, \nabla q \right\rangle \\ &= \left\langle \sum_{i=1}^N V_i \rho_{h,i}^k \mathbf{u}_h^{k+1}, \nabla q \right\rangle + \langle \operatorname{div} \mathbf{u}_h^{k+1}, q \rangle = \left\langle \left( \sum_{i=1}^N V_i \rho_{h,i}^k - 1 \right) \mathbf{u}_h^{k+1}, \nabla q \right\rangle. \end{aligned}$$

For the energy identity, we choose the test function  $\mathbf{v} = \mathbf{u}_h^{k+1}$  in (22):

$$\begin{aligned} & \frac{1}{2\tau} \langle \mathbf{u}_h^{k+1} (\rho_h^{k+1} - \rho_h^k), \mathbf{u}_h^{k+1} \rangle + \frac{1}{\tau} \langle \rho_h^k (\mathbf{u}_h^{k+1} - \mathbf{u}_h^k), \mathbf{u}_h^{k+1} \rangle + \mathbf{b}_{\text{skw}}(\rho_h^* \mathbf{u}_h^*, \mathbf{u}_h^{k+1}, \mathbf{u}_h^{k+1}) \\ & - \langle p_h^{n+1}, \operatorname{div} \mathbf{u}_h^{k+1} \rangle + \langle \mathbb{S}(\bar{\rho}_h^*, \nabla \mathbf{u}_h^{k+1}), \nabla \mathbf{u}_h^{k+1} \rangle + \sum_{i=1}^N \langle \rho_{h,i}^k \nabla (\mu_{h,i}^{k+1} - V_i p_h^{k+1}), \mathbf{u}_h^{k+1} \rangle = 0. \end{aligned} \quad (25)$$

Notice that  $\mathbf{b}_{\text{skw}}(\rho_h^* \mathbf{u}_h^*, \mathbf{u}_h^{k+1}, \mathbf{u}_h^{k+1}) = 0$ . An elementary computation shows that

$$\begin{aligned} & \frac{1}{2} (\rho_h^{k+1} - \rho_h^k) |\mathbf{u}_h^{k+1}|^2 + \rho_h^k (\mathbf{u}_h^{k+1} - \mathbf{u}_h^k) \cdot \mathbf{u}_h^{k+1} \\ &= \frac{1}{2} \rho_h^{k+1} |\mathbf{u}_h^{k+1}|^2 - \frac{1}{2} \rho_h^k |\mathbf{u}_h^k|^2 + \frac{1}{2} \rho_h^k |\mathbf{u}_h^{k+1} - \mathbf{u}_h^k|^2. \end{aligned}$$

Thus, replacing the first two terms in (25), we have

$$\begin{aligned} & \frac{1}{2\tau} \langle \rho_h^{k+1} |\mathbf{u}_h^{k+1}|^2, 1 \rangle - \frac{1}{2\tau} \langle \rho_h^k |\mathbf{u}_h^k|^2, 1 \rangle + \frac{1}{2\tau} \langle \rho_h^k |\mathbf{u}_h^{k+1} - \mathbf{u}_h^k|^2, 1 \rangle - \langle p_h^{k+1}, \operatorname{div} \mathbf{u}_h^{k+1} \rangle \\ & + \langle \mathbb{S}(\bar{\rho}_h^*, \nabla \mathbf{u}_h^{k+1}), \nabla \mathbf{u}_h^{k+1} \rangle + \sum_{i=1}^N \langle \rho_{h,i}^k \nabla (\mu_{h,i}^{k+1} - V_i p_h^{k+1}), \mathbf{u}_h^{k+1} \rangle = 0. \end{aligned} \quad (26)$$

To reformulate the fourth term, we take  $q = p_h^{k+1}$  in (23) and then  $\psi_i = V_i p_h^{k+1}$  in (20):

$$\begin{aligned} \langle p_h^{k+1}, \operatorname{div} \mathbf{u}_h^{k+1} \rangle &= - \sum_{i,j=1}^N \langle V_i M_{ij}(\bar{\rho}_h^*) \nabla \mu_{h,j}^{k+1}, \nabla p_h^{k+1} \rangle \\ &= \sum_{i=1}^N \frac{1}{\tau} \langle \rho_{h,i}^{k+1} - \rho_{h,i}^k, V_i p_h^{k+1} \rangle - \sum_{i=1}^N \langle \rho_{h,i}^k \mathbf{u}_h^{k+1}, V_i \nabla p_h^{k+1} \rangle. \end{aligned}$$

Combining (26) and the previous expression, some terms cancel:

$$\begin{aligned} & \frac{1}{2\tau} \langle \rho_h^{k+1} |\mathbf{u}_h^{k+1}|^2, 1 \rangle - \frac{1}{2\tau} \langle \rho_h^k |\mathbf{u}_h^k|^2, 1 \rangle + \frac{1}{2\tau} \langle \rho_h^k |\mathbf{u}_h^{k+1} - \mathbf{u}_h^k|^2, 1 \rangle \\ & + \langle \mathbb{S}(\bar{\rho}_h^*, \nabla \mathbf{u}_h^{k+1}), \nabla \mathbf{u}_h^{k+1} \rangle + \sum_{i=1}^N \langle \rho_{h,i}^k \nabla \mu_{h,i}^{k+1}, \mathbf{u}_h^{k+1} \rangle = \frac{1}{\tau} \sum_{i=1}^N \langle \rho_{h,i}^{k+1} - \rho_{h,i}^k, V_i p_h^{k+1} \rangle. \end{aligned} \quad (27)$$

For the internal energy contribution, we add and subtract some terms:

$$\frac{1}{\tau} \langle f(\bar{\rho}_h^{k+1}), 1 \rangle - \frac{1}{\tau} \langle f(\bar{\rho}_h^k), 1 \rangle = \frac{1}{\tau} \sum_{i=1}^N \left\langle \frac{\partial f(\bar{\rho}_h^{k+1})}{\partial \rho_i}, \rho_{h,i}^{k+1} - \rho_{h,i}^k \right\rangle \quad (28)$$

$$+ \frac{1}{\tau} \langle f(\bar{\rho}_h^{k+1}), 1 \rangle - \frac{1}{\tau} \langle f(\bar{\rho}_h^k), 1 \rangle - \frac{1}{\tau} \sum_{i=1}^N \left\langle \frac{\partial f(\bar{\rho}_h^{k+1})}{\partial \rho_i}, \rho_{h,i}^{k+1} - \rho_{h,i}^k \right\rangle.$$

The last line can be rewritten as part of the numerical dissipation  $\mathcal{D}_{\text{num}}$  using Taylor expansion. Using the definition of the discrete energy  $E_h$  and the numerical dissipation  $\mathcal{D}_{\text{num}}$ , a combination of (27) and (28) gives

$$\begin{aligned} \frac{1}{\tau} \langle E_h^{k+1} - E_h^k, 1 \rangle &= -\mathcal{D}_{\text{num}} - \langle \mathbb{S}(\bar{\rho}_h^*, \nabla \mathbf{u}_h^{k+1}), \nabla \mathbf{u}_h^{k+1} \rangle \\ &+ \frac{1}{\tau} \sum_{i=1}^N \left\langle \rho_{h,i}^{k+1} - \rho_{h,i}^k, \frac{\partial f(\bar{\rho}_h^{k+1})}{\partial \rho_i} + V_i p_h^{k+1} \right\rangle - \sum_{i=1}^N \langle \rho_{h,i}^k \nabla \mu_{h,i}^{k+1}, \mathbf{u}_h^{k+1} \rangle. \end{aligned} \quad (29)$$

We choose  $\xi_i = (\rho_{h,i}^{k+1} - \rho_{h,i}^k)/\tau$  in (21) and then  $\psi_i = \mu_{h,i}^{k+1}$  in (20) to rewrite the third term on the right-hand side:

$$\begin{aligned} \frac{1}{\tau} \sum_{i=1}^N \left\langle \rho_{h,i}^{k+1} - \rho_{h,i}^k, \frac{\partial f(\bar{\rho}_h^{k+1})}{\partial \rho_i} + V_i p_h^{k+1} \right\rangle &= \frac{1}{\tau} \sum_{i=1}^N \langle \rho_{h,i}^{k+1} - \rho_{h,i}^k, \mu_{h,i}^{k+1} \rangle \\ &= \sum_{i=1}^N \langle \rho_{h,i}^k \mathbf{u}_h^{k+1}, \nabla \mu_{h,i}^{k+1} \rangle - \sum_{i,j=1}^N \langle M_{i,j}(\bar{\rho}_h^*) \nabla \mu_{h,i}^{k+1}, \nabla \mu_{h,j}^{k+1} \rangle. \end{aligned}$$

The first term on the right-hand side cancels with the last term in (29). This shows that

$$\frac{1}{\tau} \langle E_h^{k+1} - E_h^k, 1 \rangle = -\mathcal{D}_{\text{num}} - \langle \mathbb{S}(\bar{\rho}_h^*, \nabla \mathbf{u}_h^{k+1}), \nabla \mathbf{u}_h^{k+1} \rangle - \sum_{i,j=1}^N \langle M_{i,j}(\bar{\rho}_h^*) \nabla \mu_{h,i}^{k+1}, \nabla \mu_{h,j}^{k+1} \rangle,$$

which finishes the proof.

Assumptions (A0)–(A4) imply some pointwise bounds and bounds in  $L^2(\Omega)$ .

**Theorem 2 (A priori bounds)** *Let Assumptions (A0)–(A4) hold and let  $(\bar{\rho}_h^k, \mathbf{u}_h^k) \in \Pi_\tau^1(\mathcal{V}_{h,+}^N \times \mathcal{X}_h^d)$ ,  $(\bar{\mu}_h^k, p_h^k) \in \Pi_\tau^0(\mathcal{V}_h^N \times \mathcal{Q}_h)$  be a solution to (20)–(23). Then, for all  $k = 1, \dots, n$ :*

– *Pointwise constraint:*

$$\sum_{i=1}^N V_i \rho_{h,i}^k(x) = 1 \quad \text{for all } x \in \Omega.$$

– *Pointwise bounds:*

$$\rho_{h,i}^k \leq V_i^{-1} \quad \text{for } i = 1, \dots, N, \quad V_{\max}^{-1} \leq \rho_h^k \leq V_{\min}^{-1},$$

where  $V_{\min} = \min\{V_1, \dots, V_N\}$  and  $V_{\max} = \max\{V_1, \dots, V_N\}$ .

– *A priori estimates:*

$$\max_{k=1, \dots, n} (\|\mathbf{u}_h^k\|_{L^2(\Omega)}^2 + \|(\rho_h^k)^{1/2} \mathbf{u}_h^k\|_{L^2(\Omega)}^2) + \sum_{k=1}^n \tau \|\nabla \mathbf{u}_h^k\|_{L^2(\Omega)}^2 \leq C(E_h^0),$$

Bounds for the gradients of the partial mass densities strongly depend on the structure of the mobility matrix  $(M_{ij}(\bar{\rho}_h^k))$ . Matrix analysis arguments show for the continuous Maxwell–Stefan system that the mass densities are bounded in  $H^1(\Omega)$  [20, Lemma 3.2].

*Proof* Set  $Z_h^k := \sum_{i=1}^N V_i \rho_{h,i}^k - 1$ . Assumption (A4) implies that  $Z_h^0 = 0$ . By partial mass conservation,  $\langle V_i \rho_{h,i}^k, 1 \rangle = \langle V_i \rho_{h,i}^0, 1 \rangle$  for all  $i = 1, \dots, N$  and  $k = 1, \dots, n$ . Summation over  $i = 1, \dots, N$  shows that

$$\langle Z_h^k, 1 \rangle = \left\langle \sum_{i=1}^N V_i \rho_{h,i}^k - 1, 1 \right\rangle = \left\langle \sum_{i=1}^N V_i \rho_{h,i}^0 - 1, 1 \right\rangle = \langle Z_h^0, 1 \rangle = 0.$$

Equation (24) writes as

$$\langle Z_h^{k+1}, q \rangle - \langle Z_h^k, q \rangle = \tau \langle Z_h^k \mathbf{u}_h^{k+1}, \nabla q \rangle,$$

which reduces with the test function  $q = Z_h^1$  to

$$\|q\|_{L^2(\Omega)}^2 = \langle Z_h^1, q \rangle - \langle Z_h^0, q \rangle = \tau \langle Z_h^0 \mathbf{u}_h^1, \nabla q \rangle = 0,$$

proving that  $q = Z_h^1 = 0$  a.e. in  $\Omega$ . The first assertion follows after an induction argument.

Next, the upper bound for  $\rho_{h,i}^k$  follows from  $V_j \rho_{h,j}^k = 1 - \sum_{i \neq j} V_i \rho_{h,i}^k \leq 1$ , using the nonnegativity of  $\rho_{h,i}^k$ . The bounds for the total mass density is a consequence of

$$\frac{1}{V_{\max}} = \sum_{i=1}^N \frac{V_i}{V_{\max}} \rho_{h,i}^k \leq \sum_{i=1}^N \rho_{h,i}^k \leq \sum_{i=1}^N \frac{V_i}{V_{\min}} \rho_{h,i}^k = \frac{1}{V_{\min}}.$$

Finally, the discrete energy identity from Theorem 1 and Assumption (A3) imply directly the a priori estimates.

### 3.3 Remarks

We discuss some variants of the numerical scheme.

*Remark 1 (Implicit discretization in (20))* Observe that the choice of the old time step  $\rho_{h,i}^k$  in the transport term of (20) allows us to derive the pointwise form of the constraint. A similar result can be proven for the implicit discretization, i.e. replacing  $\rho_{h,i}^k \mathbf{u}_h^{k+1}$  by  $\rho_{h,i}^{k+1} \mathbf{u}_h^{k+1}$  in (20) under the assumption that all mass densities  $\rho_{h,i}^k$  are uniformly positive independently of the time step  $\tau$  and under a CFL-type condition. Indeed, similarly as in the previous proof, we find that

$$\langle Z_h^1, q \rangle - \langle Z_h^0, q \rangle = \tau \langle Z_h^1 \mathbf{u}_h^1, \nabla q \rangle,$$

and the choice  $q = Z_h^1$  leads to

$$\|q\|_{L^2(\Omega)}^2 = \frac{\tau}{2} \langle \mathbf{u}_h^1, \nabla |Z_h^1|^2 \rangle = -\frac{\tau}{2} \langle \operatorname{div} \mathbf{u}_h^1, |Z_h^1|^2 \rangle \leq \frac{\tau}{2} \|\operatorname{div} \mathbf{u}_h^1\|_{L^2(\Omega)} \|Z_h^1\|_{L^2(\Omega)}^2.$$

It follows from the inverse inequality for finite element functions between the spaces  $W^{1,\infty}(\Omega)$  and  $L^2(\Omega)$  that

$$\|q\|_{L^2(\Omega)}^2 \leq C \tau h^{-1-d/2} \|\mathbf{u}_h^1\|_{L^2(\Omega)} \|Z_h^1\|_{L^2(\Omega)}^2 \leq C_0 \tau h^{-1-d/2} \|q\|_{L^2(\Omega)}^2.$$

We infer from the CFL-type condition  $\tau h^{-1-d/2} < 1/C_0$  that  $\|q\|_{L^2(\Omega)}^2 = 0$  and hence  $Z_h^1 = 0$ .

*Remark 2 (Equal specific volumes)* In the case  $V_i = V$  for  $i = 1, \dots, N$ , the numerical scheme simplifies. Indeed, we obtain  $1 = \sum_{i=1}^N V_i \rho_{h,i}^k = V \rho_h^k$  and hence  $\rho_h^k = V^{-1}$ . Next, we choose the test function  $\psi_i = \psi \in \mathcal{V}_h$  in (20), sum over  $i = 1, \dots, N$ , and use  $\sum_{i=1}^N M_{ij}(\bar{\rho}_h^*) = 0$ :

$$\langle V^{-1} \mathbf{u}_h^{k+1}, \nabla \psi \rangle = -\frac{1}{\tau} \sum_{i=1}^N \langle \rho_{h,i}^{k+1} - \rho_{h,i}^k, \psi \rangle + \sum_{i,j=1}^n \langle M_{ij}(\bar{\rho}_h^*) \nabla \mu_{h,j}^{k+1}, \nabla \psi \rangle = 0,$$

which yields  $\langle \mathbf{u}_h^{k+1}, \nabla \psi \rangle = 0$  for all  $\psi \in \mathcal{V}_h$ . The discrete momentum equation (22) then becomes for  $\mathbf{v} \in \mathcal{X}_h^d$ :

$$\begin{aligned} & \langle \rho(\mathbf{u}_h^{k+1} - \mathbf{u}_h^k), \mathbf{v} \rangle + \mathbf{b}_{\text{skw}}(\rho \mathbf{u}_h^*, \mathbf{u}_h^{k+1}, \mathbf{v}) - \langle p_h^{k+1}, \text{div} \mathbf{v} \rangle \\ & + \langle \mathbb{S}(\bar{\rho}_h^*, \nabla \mathbf{u}_h^{k+1}), \nabla \mathbf{v} \rangle + \sum_{i=1}^N \langle \rho_{h,i}^k \nabla(\mu_{h,i}^{k+1} - V_i p_h^{k+1}), \mathbf{v} \rangle = 0. \end{aligned}$$

We claim that we can formulate a nodal representation in which the pressure does not appear. For this, let  $(\phi_\ell)$  be a (finite-dimensional) basis of  $\mathcal{V}_h$ , let  $L_{\ell m} = \langle \phi_\ell, \phi_m \rangle$  be the entries of the mass matrix  $\mathbb{L}$ ,  $K_{ij, \ell m}^* = \langle M_{ij}(\bar{\rho}_h^*) \nabla \phi_\ell, \nabla \phi_m \rangle$  be the entries of the weighted stiffness matrix  $\mathbb{K}_{ij}^*$ , and  $F_{i,j}^k = \langle (\partial f / \partial \rho_i)(\bar{\rho}_h^k), \phi_j \rangle$  be the entries of the nonlinear term  $\mathbf{F}_i^k$ . Slightly abusing our notation, we set  $\boldsymbol{\mu}_i^k = \langle \mu_{h,i}^k, \phi_\ell \rangle_\ell$  and  $\mathbf{p}^k = \langle p_h^k, \phi_\ell \rangle_\ell$ . Then (21) becomes

$$\boldsymbol{\mu}_i^k = \mathbb{L}^{-1} \mathbf{F}_i^k + V \mathbf{p}^k \quad \text{for } i = 1, \dots, N$$

and consequently,

$$\sum_{j=1}^n \langle M_{ij}(\bar{\rho}_h^*) \nabla \mu_{h,j}^k, \nabla \phi_i \rangle_\ell = \sum_{j=1}^N \mathbb{K}_{ij}^* \boldsymbol{\mu}_j^k = \sum_{j=1}^N \mathbb{K}_{ij}^* (\mathbb{L}^{-1} \mathbf{F}_j^k + V \mathbf{p}^k) = \sum_{j=1}^N \mathbb{K}_{ij}^* \mathbb{L}^{-1} \mathbf{F}_j^k,$$

where the last step follows from the fact that the sum over the entries of the mobility matrix vanishes. Then, defining  $\hat{\boldsymbol{\mu}}_j^k = \mathbb{L}^{-1} \mathbf{F}_j^k$ ,

$$\sum_{j=1}^n \langle M_{ij}(\bar{\rho}_h^*) \nabla \mu_{h,j}^k, \nabla \phi_\ell \rangle = \sum_{j=1}^n \langle M_{ij}(\bar{\rho}_h^*) \nabla \hat{\boldsymbol{\mu}}_j^k, \nabla \phi_\ell \rangle,$$

which means that we can replace  $\boldsymbol{\mu}_j^k$  by  $\hat{\boldsymbol{\mu}}_j^k$ . Furthermore, introducing the matrix  $\mathbb{G}(\rho_{h,i}^k)$  with entries  $G_{\ell m}(\rho_{h,i}^k) = \langle \rho_{h,i}^k \nabla \phi_\ell, \nabla \phi_m \rangle$  and inserting the vector equation for  $\boldsymbol{\mu}_i^k$ ,

$$\begin{aligned} \sum_{i=1}^N \langle \rho_{h,i}^k (\nabla \mu_{h,i}^k - V \nabla p_h^k), \mathbf{v} \rangle &= \sum_{i=1}^N \mathbb{G}(\rho_{h,i}^k) (\boldsymbol{\mu}_i^k - V \mathbf{p}^k) \mathbf{v} \\ &= \sum_{i=1}^N \mathbb{G}(\rho_{h,i}^k) \mathbb{L}^{-1} \mathbf{F}_i^k \mathbf{v} = \sum_{i=1}^N \langle \rho_{h,i}^k \nabla \hat{\boldsymbol{\mu}}_{h,i}^k, \mathbf{v} \rangle. \end{aligned}$$

Thus, only  $\hat{\boldsymbol{\mu}}_i^k$  appears in the incompressible Navier–Stokes–Maxwell–Stefan equations instead of  $\boldsymbol{\mu}_i^k$ .

## 4 Numerical experiments

In this section, we present some numerical simulations in two space dimensions, illustrating the convergence of the scheme and the structure-preserving properties. The scheme is implemented in NGSolve [25], using Netgen for the generation of an unstructured mesh of triangles. The resulting nonlinear system is solved by Newton’s method with a tolerance of  $10^{-9}$  (measured in the  $L^2(\Omega)$  norm), and the linear systems are computed via direct LU decomposition. In all tests, we fixed the computational domain  $\Omega = (0, 1)^2$  with periodic boundary conditions. This means that we identify  $\Omega$  with the two-dimensional torus.

## 4.1 Convergence tests

We consider  $N = 2$  components, the final time  $T = 0.1$ , and the stress tensor  $\mathbb{S}(\nabla \mathbf{u}) = \nu(\nabla \mathbf{u}^T + \nabla \mathbf{u}) + \lambda(\operatorname{div} \mathbf{u})\mathbb{I}$  with  $\nu = 10^{-3}$  and  $\lambda = 0$ . The internal energy density is chosen as  $f(\vec{\rho}) = \sum_{i=1}^2 \rho_i \log(\rho_i/\rho)$ , and the mobility matrix is given by (5), i.e.  $M_{ij}(\vec{\rho}) = \rho_i \delta_{ij} - \rho_i \rho_j / \rho$ . The initial data equals

$$\begin{aligned} \rho_1^0(x, y) &= 1 + 0.8 \sin(4\pi x) \sin(2\pi y), & \rho_2^0(x, y) &= V_2^{-1}(1 - V_1 \rho_1^0(x, y)), \\ \mathbf{u}^0(x, y) &= \left( -\sin(\pi x)^2 \sin(2\pi y), \sin(2\pi x) \sin(\pi y)^2 \right)^T. \end{aligned}$$

Since no exact solution is available, we compute the error by using the reference solution at the finest space resolution. Given the mesh sizes  $h_k = 2^{-k-1}$  for  $k = 0, \dots, 7$  and  $h_{\text{ref}} = 2^{-7}$ , we define the error quantities

$$\begin{aligned} \operatorname{err}(\vec{\rho}) &= \max_{k=1, \dots, n} \sum_{i=1}^2 \|\rho_{h_k, i}^k - \rho_{\text{ref}, i}^k\|_{L^2(\Omega)}^2, & \operatorname{err}(\vec{\mu}) &= \tau \sum_{k=1}^n \sum_{i=1}^2 \|\mu_{h_k, i}^k - \mu_{\text{ref}, i}^k\|_{L^2(\Omega)}^2, \\ \operatorname{err}(\mathbf{u}) &= \max_{k=1, \dots, n} \|\mathbf{u}_{h_k}^k - \mathbf{u}_{\text{ref}}^k\|_{L^2(\Omega)}^2, & \operatorname{err}(p) &= \tau \sum_{k=1}^n \|p_{h_k}^k - p_{\text{ref}}^k\|_{L^2(\Omega)}^2. \end{aligned}$$

We have chosen the time step size  $\tau = 10^{-3}$  such that  $n = T/\tau = 100$ . Table 1 presents the errors and the (squared) experimental order of convergence for  $V_1 = 0.3$ ,  $V_2 = 0.7$ , while Table 2 shows these values for the choice  $V_1 = V_2 = 0.5$ . As expected, we observe second-order convergence for  $(\vec{\rho}, \vec{\mu}, p)$  and second-order convergence for  $\mathbf{u}$  (recall that the velocity is approximated by piecewise quadratic polynomials, for which third-order might be possible). In the second test case, the order of convergence for the pressure is larger than in the first test, which comes from the choice  $V_1 = V_2$ , i.e., we have solved the incompressible Navier–Stokes equations. In both tests, the partial and total masses and the pointwise quasi-incompressibility constraint are conserved up to errors of order  $10^{-14}$ .

**Table 1**  $L^2(\Omega)$  errors and squared experimental order of convergence (eoc) for  $V_1 = 0.3$ ,  $V_2 = 0.7$ .

$k$	$\operatorname{err}(\vec{\rho})$	eoc	$\operatorname{err}(\vec{\mu})$	eoc	$\operatorname{err}(\mathbf{u})$	eoc	$\operatorname{err}(p)$	eoc
1	$5.31 \cdot 10^{-2}$	–	$3.04 \cdot 10^{-3}$	–	$1.42 \cdot 10^{-1}$	–	$5.67 \cdot 10^{-3}$	–
2	$7.90 \cdot 10^{-2}$	–0.57	$4.74 \cdot 10^{-3}$	–0.63	$6.02 \cdot 10^{-3}$	4.56	$8.81 \cdot 10^{-3}$	–0.63
3	$6.83 \cdot 10^{-3}$	3.53	$6.15 \cdot 10^{-4}$	2.95	$1.48 \cdot 10^{-3}$	2.02	$9.94 \cdot 10^{-4}$	3.15
4	$3.75 \cdot 10^{-4}$	4.18	$4.47 \cdot 10^{-5}$	3.78	$1.96 \cdot 10^{-4}$	2.90	$6.60 \cdot 10^{-5}$	3.91
5	$2.36 \cdot 10^{-5}$	4.00	$2.85 \cdot 10^{-6}$	3.97	$1.40 \cdot 10^{-5}$	3.82	$4.18 \cdot 10^{-6}$	3.98
6	$1.42 \cdot 10^{-6}$	4.04	$1.69 \cdot 10^{-7}$	4.07	$4.66 \cdot 10^{-7}$	4.91	$2.49 \cdot 10^{-7}$	4.07
7	$9.24 \cdot 10^{-8}$	3.94	$1.12 \cdot 10^{-8}$	3.91	$1.57 \cdot 10^{-8}$	4.89	$1.64 \cdot 10^{-8}$	3.92

**Table 2**  $L^2(\Omega)$  errors and squared experimental order of convergence (eoc) for  $V_1 = V_2 = 0.5$ .

$k$	$\operatorname{err}(\vec{\rho})$	eoc	$\operatorname{err}(\vec{\mu})$	eoc	$\operatorname{err}(\mathbf{u})$	eoc	$\operatorname{err}(p)$	eoc
1	$8.96 \cdot 10^{-2}$	–	$8.14 \cdot 10^{-3}$	–	$1.37 \cdot 10^{-1}$	–	$1.46 \cdot 10^{-2}$	–
2	$1.33 \cdot 10^{-1}$	–0.57	$6.81 \cdot 10^{-3}$	0.26	$4.84 \cdot 10^{-4}$	8.15	$1.10 \cdot 10^{-2}$	0.42
3	$1.15 \cdot 10^{-2}$	3.53	$2.16 \cdot 10^{-4}$	4.97	$3.55 \cdot 10^{-5}$	3.77	$4.41 \cdot 10^{-5}$	7.96
4	$6.36 \cdot 10^{-4}$	4.18	$1.71 \cdot 10^{-5}$	3.66	$6.26 \cdot 10^{-6}$	2.50	$4.78 \cdot 10^{-7}$	6.53
5	$3.87 \cdot 10^{-5}$	4.04	$1.10 \cdot 10^{-6}$	3.96	$4.30 \cdot 10^{-7}$	3.86	$1.41 \cdot 10^{-8}$	5.09
6	$2.33 \cdot 10^{-6}$	4.05	$6.74 \cdot 10^{-8}$	4.02	$1.43 \cdot 10^{-8}$	4.90	$7.33 \cdot 10^{-10}$	4.23
7	$1.56 \cdot 10^{-7}$	3.90	$4.51 \cdot 10^{-9}$	3.90	$2.89 \cdot 10^{-10}$	5.63	$4.80 \cdot 10^{-11}$	3.93

## 4.2 Three-component experiment I

We present a numerical test for  $N = 3$  components based on a similar test in [8, Sec. 5.2]. We choose the stress tensor as in the previous section with  $\nu = 10^{-2}$  and  $\lambda = 0$ , the internal energy density  $f(\vec{\rho}) = \sum_{i=1}^3 \rho_i \log(\rho_i/\rho)$ , and the mobility matrix (5), i.e.  $M_{ij}(\vec{\rho}) = \rho_i \delta_{ij} - \rho_i \rho_j / \rho$ . The specific volumes are  $V_1 = V_2 = 0.35$  and  $V_3 = 0.8$ . The final time is set to  $T = 0.5$ , the time step size equals  $\tau = 10^{-4}$ , and the maximal mesh size is  $h = 2^{-7}$ . The initial data reads as

$$\begin{aligned} \rho_1^0(x, y) &= 0.2 + 0.9\chi(x, y, y \in [0.1, 0.2] \cup (0.8, 0.9]) + 0.9\chi(x, y, x \in [0.1, 0.2] \cup (0.8, 0.9]) \\ &\quad - 0.9\chi(x, y, (x, y) \in ((0.1, 0.2] \times ([0.1, 0.2] \cup [0.8, 0.9]))) \\ &\quad - 0.9\chi(x, y, (x, y) \in ([0.1, 0.2] \cup [0.8, 0.9]) \times (0.1, 0.2)), \\ \rho_2^0(x, y) &= 0.2 + 0.9\chi(x, y, (x, y) \in \{(x - 0.5)^2 + (y - 0.5)^2 - 0.25^2 \leq 0\}), \\ \rho_3^0(x, y) &= V_3^{-1}(1 - V_1\rho_1(x, y) - V_2\rho_2(x, y)), \\ \mathbf{u}(x, y) &= (-\sin(\pi x)^2 \sin(2\pi y), \sin(\pi y)^2 \sin(2\pi x))^T, \end{aligned}$$

where  $\chi(x, y, y \in I)$  is the characteristic function on  $[0, 1] \times I$ , and similarly for the other functions. Figures 1–2 illustrate the time evolution of the partial mass densities  $\rho_i$ , total mass  $\rho$ , velocity magnitude  $|\mathbf{u}|^2$ , and pressure  $p$ . The coupling to the Navier–Stokes equations induces rotating shapes before the mass densities converge to the homogeneous steady state. The intermediate state is different from the numerical results of the Maxwell–Stefan equations presented in [8, Sec. 5.2], where the mass densities only diffuse and do not show any rotational effect.

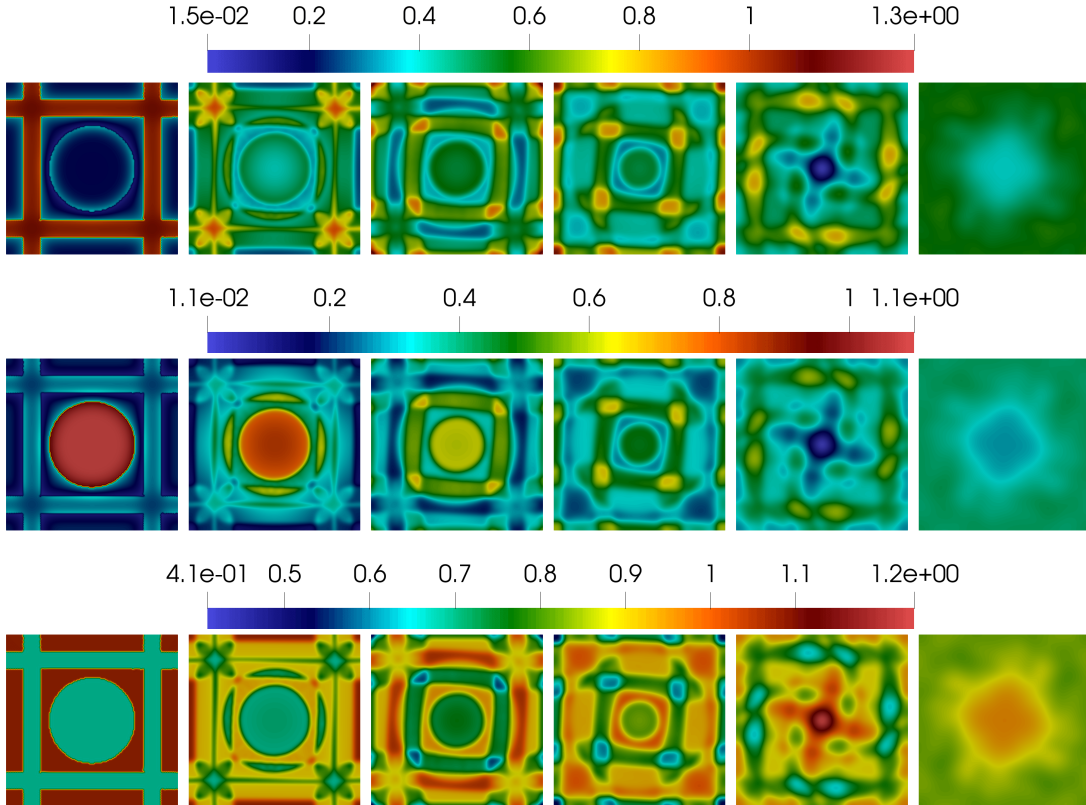


**Fig. 1** Snapshots of the partial mass densities  $\rho_1$  (upper row),  $\rho_2$  (middle row), and  $\rho_3$  (lower row) at times  $t = 0.001, 0.02, 0.04, 0.06, 0.1, 0.5$ .

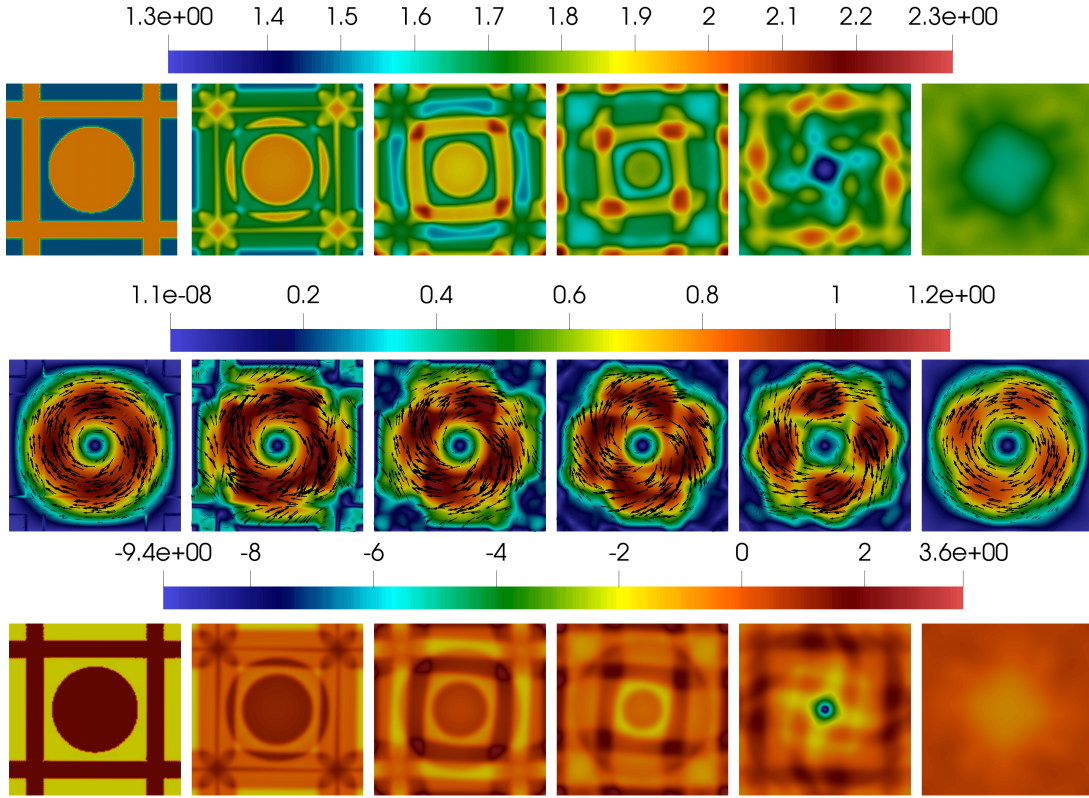


**Fig. 2** Snapshots of the total mass density  $\rho$  (upper row), velocity magnitude  $|\mathbf{u}|^2$ , and pressure  $p$  at times  $t = 0.001, 0.02, 0.04, 0.06, 0.1, 0.5$ .

Figure 3 shows the time decay of the discrete variant of the relative energy

$$\int_{\Omega} \left( \sum_{i=1}^n \rho_i \log \frac{\rho_i}{\rho_i^{\infty}} - \rho \log \frac{\rho}{\rho^{\infty}} + \frac{\rho}{2} |\mathbf{u} - \mathbf{u}^{\infty}|^2 \right) dx,$$

where the stationary variables are defined by

$$\rho_i^{\infty} = \langle \rho_i^0, 1 \rangle, \quad \mathbf{u}^{\infty} = \frac{\langle \rho^0 \mathbf{u}^0, 1 \rangle}{\langle \rho^0, 1 \rangle}.$$

Moreover,  $\rho^{\infty} := \sum_{i=1}^N \rho_i^{\infty}$  is the stationary total mass, and the stationary pressure vanishes,  $p^{\infty} = 0$ . The relative energy is computed by NGSolve by using a fifth-order quadrature rule. We observe that the relative energy decays with time (nearly exponentially for large times). Interestingly, the components of the relative energy (the relative internal energy and the relative kinetic energy) do not decrease in time, but only its sum. This is in contrast to the incompressible Navier–Stokes–Maxwell–Stefan model, where the kinetic and internal energies are both decaying in time. This is not surprising, since in that model, the Maxwell–Stefan diffusion and Navier–Stokes flow are basically decoupled, while the coupling is much stronger in our model. Again the partial and total masses and the pointwise quasi-incompressibility constraint are conserved up to errors of order  $10^{-14}$ .

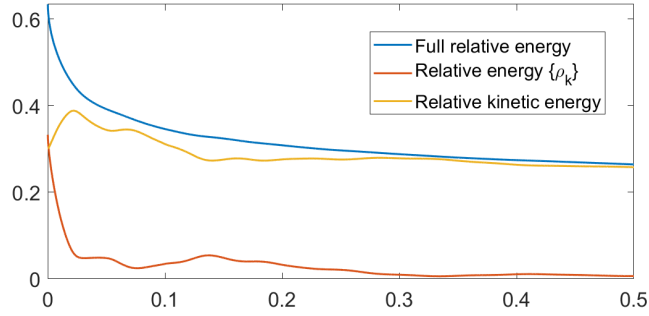


**Fig. 3** Relative energy versus time.

#### 4.3 Three-component experiment II

We present a second three-component experiment with the same data as in the previous subsection, except  $\eta = 10^{-1}$ ,  $M_{ij}(\vec{\rho}) = 10^{-1}(\rho_i \delta_{ij} - \frac{\rho_i \rho_j}{\rho})$ ,  $V_1 = 0.35$ ,  $V_2 = 0.65$ ,  $V_3 = 0.5$  and

$$\begin{aligned} \rho_1^0(x, y) &= 0.5 + 0.49999 \tanh\left(\frac{\sqrt{(x-0.4)^2 + (y-0.4)^2} - 0.25}{10^{-2}\sqrt{2}}\right), \\ \rho_2^0(x, y) &= 0.5 + 0.49999 \tanh\left(\frac{\sqrt{(x-0.6)^2 + (y-0.6)^2} - 0.25}{10^{-2}\sqrt{2}}\right), \\ \rho_3^0(x, y) &= V_3^{-1}(1 - V_1\rho_1(x, y) - V_2\rho_2(x, y)), \\ \mathbf{u}^0(x, y) &= (-\sin(\pi x)^2 \sin(2\pi y), \sin(\pi y)^2 \sin(2\pi x))^T. \end{aligned}$$

Compared to the previous test, the effect of the initial velocity can be observed much better. Figure 4 illustrates the dynamics of the partial and total mass densities at various times. Again, the mass densities diffuse over time and show some rotational effect, which is well seen for the component  $\rho_3$ .

## 5 Conclusion and outlook

We have derived and analyzed a new structure-preserving finite element scheme for the Navier–Stokes–Maxwell–Stefan equations with a generalized incompressibility constraint. After a suitable variational formulation of the continuous problem, the space discretization is realized by a conforming piecewise linear/quadratic finite element approximation. The time discretization is of mixed explicit–implicit type, allowing us to prove that the quasi-incompressibility constraint is satisfied pointwise in space. The resulting numerical scheme conserves the partial and total masses and satisfies a discrete energy inequality with a nonnegative numerical dissipation term. Convergence tests for a two-component mixture verify the expected convergence orders and structure-preserving properties. The numerical tests for a three-component mixture exhibit some rotational behavior of the mass densities, which is absent in the incompressible model.

Future work will be concerned with the existence analysis of the numerical scheme and the proof of the positivity of the mass densities. One approach is to use the reformulation of the problem from [11] in terms of the so-called relative chemical potentials. A critical part of the proof is the  $L^1(\Omega)$  bound for the pressure, since the proof in [11, Prop. 7.4] relies on the (continuous) Bogovski operator. The hope is that the discrete counterpart of this operator can be used; see [22]. The (local-in-time) proof of [3] does not use the Bogovski operator and may provide another approach to prove the existence of discrete solutions.

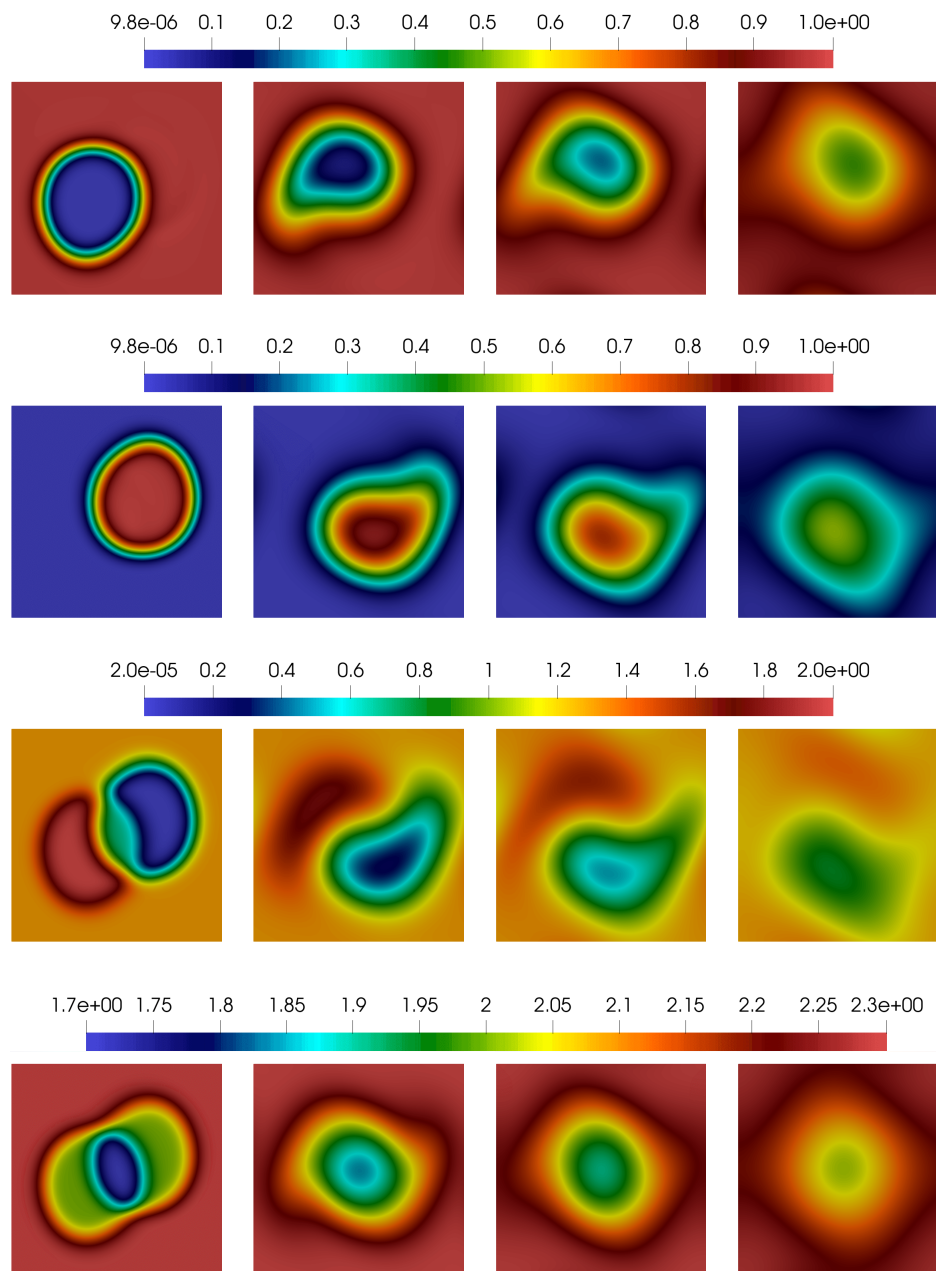


**Fig. 4** Snapshots of the partial mass densities  $\rho_1$  (first row),  $\rho_2$  (second row),  $\rho_3$  (third row) and the total mass density  $\rho$  (last row) at times  $t = 0.1, 0.6, 1, 2$ .

#### Data availability statement

This study did not generate or analyze any datasets. Therefore, data sharing is not applicable to this work.

#### Declarations

The authors declare that they have no conflict of interest.

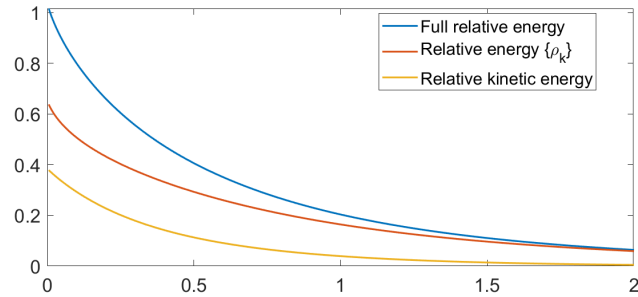


Fig. 5 Relative energy versus time.

## References

1. F. Aznaran, P. Farrell, C. Monroe, and A. Van-Brunt. Finite element methods for multicomponent convection-diffusion. *IMA J. Numer. Anal.* 45 (2025), 188–222.
2. D. Bothe. On the Maxwell–Stefan equations to multicomponent diffusion. In: J. Escher et al. (eds.), *Progress in Nonlinear Differential Equations and their Applications*, pp. 81–93. Springer, Basel, 2011.
3. D. Bothe and P.-E. Druet. Well-posedness analysis of multicomponent incompressible flow models. *J. Evol. Eqs.* 21 (2021), 4039–4093.
4. D. Bothe and P.-E. Druet. On the structure of continuum thermodynamical diffusion fluxes—A novel closure scheme and its relation to the Maxwell–Stefan and the Fick–Onsager approach. *Int. J. Eng. Sci.* 184 (2023), no. 103818, 33 pages.
5. D. Bothe and J. Prüss. Modeling and analysis of reactive multi-component two-phase flows with mass transfer and phase transition – the isothermal incompressible case. *Discrete Contin. Dyn. Sys. S* 10 (2017), 673–696.
6. L. Boudin, B. Grec, and F. Salvarani. A mathematical and numerical analysis of the Maxwell–Stefan diffusion equations. *Discrete Contin. Dyn. Sys. B* 17 (2012), 1427–1440.
7. M. Braukhoff, I. Perugia, and P. Stocker. An entropy structure preserving space-time formulation for cross-diffusion systems: Analysis and Galerkin discretization. *SIAM J. Numer. Anal.* 60 (2022), 364–395.
8. C. Cancès, V. Ehrlacher, and L. Monasse. Finite volumes for the Stefan–Maxwell cross-diffusion system. *IMA J. Numer. Anal.* 44 (2024), 1029–1060.
9. X. Chen and A. Jüngel. Analysis of an incompressible Navier–Stokes–Maxwell–Stefan system. *Commun. Math. Phys.* 340 (2015), 471–497.
10. M. Dolce and D. Donatelli. Artificial compressibility method for the Navier–Stokes–Maxwell–Stefan system. *J. Dyn. Differ. Eqs.* 33 (2021), 35–62.
11. P.-E. Druet. Global-in-time existence for liquid mixtures subject to a generalised incompressibility constraint. *J. Math. Anal. Appl.* 499 (2021), no. 125059, 56 pages.
12. E. Feireisl, Y. Lu, and J. Márek. On PDE analysis of flows of quasi-incompressible fluids. *Z. Angew. Math. Mech.* 96 (2016), 491–508.
13. E. Feireisl and A. Novotný. *Singular Limits in Thermodynamics of Viscous Fluids*. Birkhäuser, Basel, 2009.
14. J. Geiser. Iterative solvers for the Maxwell–Stefan diffusion equations: Methods and applications in plasma and particle transport. *Cogent Math.* 2 (2015), no. 1092913, 17 pages.
15. S. Georgiadis and A. Jüngel. Global existence of weak solutions and weak–strong uniqueness for nonisothermal Maxwell–Stefan systems. *Nonlinearity* 37 (2024), no. 075016, 33 pages.
16. J. Giesselmann and J. Pryer. Energy consistent discontinuous Galerkin methods for a quasi-incompressible diffusive two phase flow model. *ESAIM: Math. Mod. Numer. Anal.* 49 (2015), 275–301.
17. C. Helmer and A. Jüngel. Analysis of Maxwell–Stefan systems for heat conducting fluid mixtures. *Nonlin. Anal. Real World Appl.* 59 (2021), no. 103263, 19 pages.
18. X. Huo, H. Liu, A. Tzavaras, and S. Wang. An energy stable and positivity-preserving scheme for the Maxwell–Stefan diffusion system. *SIAM J. Numer. Anal.* 59 (2021), 2321–2345.
19. H. Hutridurga and F. Salvarani. Existence and uniqueness analysis of a non-isothermal cross-diffusion system of Maxwell–Stefan type. *Appl. Math. Lett.* 75 (2018), 108–113.
20. A. Jüngel and I. Stelzer. Existence analysis of Maxwell–Stefan systems for multicomponent mixtures. *SIAM J. Math. Anal.* 45 (2013), 2421–2440.
21. A. Jüngel and A. Zurek. A discrete boundedness-by-entropy method for finite-volume approximations of cross-diffusion systems. *IMA J. Numer. Anal.* 43 (2023), 560–589.
22. S. Ko, P. Pustějovská, and E. Süli. Finite element approximation of an incompressible chemically reacting non-Newtonian fluid. *ESAIM: Math. Model. Numer. Anal.* 52 (2018), 509–541.
23. M. Marion and R. Temam. Global existence for fully nonlinear reaction–diffusion systems describing multicomponent reactive flows. *J. Math. Pures Appl.* 104 (2015), 102–138.
24. M. McLeod and Y. Bourgault. Mixed finite element methods for addressing multi-species diffusion using the Maxwell–Stefan equations. *Comput. Methods Appl. Mech. Eng.* 279 (2014), 515–535.
25. J. Schöberl. C++11 Implementation of Finite Elements in NGSolve. Preprint, TU Wien, Austria, 2014. <http://hdl.handle.net/20.500.12708/28346>.